PHYSICAL REVIEW B VOLUME 44, NUMBER 13 1 OCTOBER 1991-I

Late-time theory for the effects of a conserved field on the kinetics of an order-disorder transition

K. R. Elder, B. Morin, and Martin Grant
Department of Physics, McGill University, Rutherford Building, 3600 University Street, Montréal, Québec, Canada H3A 2T8

R. C. Desai
Department of Physics, University of Toronto, Toronto, Ontario, Canada M5S 1A7

(Received 15 March 1991)

The dynamics of an order-disorder transition is investigated through a nonlinear Langevin model known as model C. This model describes the dynamics of an ordering nonconserved field (e.g., sublattice concentration), ϕ, coupled to a nonordering conserved field (e.g., absolute concentration), c. An approximate asymptotic time-dependent solution is presented for both fields through a singular perturbative solution of the coupled nonlinear-dynamical system. In particular, analytic expressions for the dynamic structure factors [i.e., $S_\phi(k,t) \equiv \langle \phi(\mathbf{k},t)\phi^*(\mathbf{k},t) \rangle$, and $S_c(k,t) \equiv \langle c(\mathbf{k},t)c^*(\mathbf{k},t) \rangle$, where k is the wave vector and t is time] of both fields are presented. In the late-time regime these expressions reduce to the scaling forms $S_\phi(k,t) \approx t^{d/2} f_\phi(Q)$ and $S_c(k,t) \approx t^{d/2-1} f_c(Q)$, where $Q = kt^{1/2}$. Furthermore it is shown that $f_\phi(Q) \propto Q^{-d-1}$, $f_c(Q) \propto Q^{-d+1}$ for $Q \gg 1$ and $f_c(Q) \propto Q^4$ for $Q \ll 1$. Intermediate-time corrections, due to a finite interfacial width, to the asymptotic solutions of both fields are also obtained. Many of these predictions are experimentally accessible.

I. INTRODUCTION

The understanding of the dynamics of phase separation has been greatly enhanced by the concept of dynamical scaling.[1] The purpose of this work is to examine the scaling behavior of a model of phase separation for a nonconserved ordering field coupled to a nonordering conserved field, known as model C in the Halperin-Hohenberg classification scheme.[2] The scaling hypothesis asserts that the growth of individual phases (ψ) (e.g., concentration in binary alloy systems) from a homogeneous initial state is a function of one scaling length, the average domain size, $D \propto t^n$, where t is time and n is the growth exponent. Verification of this hypothesis has been possible due to its relatively simple predictions for readily accessible quantities in numerical and experimental studies. In particular the scaling conjecture directly implies that the time-dependent structure factor, $[S(k,t) \equiv \langle \psi(\mathbf{k},t)\psi^*(\mathbf{k},t) \rangle]$ takes the scaling form

$$S(k,t) \propto t^{dn} f(kt^n) , \tag{1}$$

where d is the dimension, k is the wave vector, and f is the scaling function. Equation (1) is valid at late times when D is much larger than any nonscaling lengths (e.g., the interfacial width W) encountered in the process. The dynamic scaling exponent n is thought to be universal and has been used to delineate universality classes. It takes the value $n = \frac{1}{2}$ for nonconserved systems[3-15] and $\frac{1}{3}$ for conserved systems.[5,8-10,16-19] Although these results are still somewhat controversial, mounting evidence seems to confirm the existence of these universality classes. In the following pages an asymptotic solution to Model C is presented and employed to determine the growth exponent and scaling functions for both fields. Care is taken to include the interfacial structure so that early-time corrections to the scaling behavior can be explicitly determined.

This solution provides a description of both long- (i.e., scaling lengths, $k \approx 2\pi/D$) and short- (i.e., nonscaling lengths $k \approx 2\pi/W$) wavelength fluctuations for the conserved and nonconserved fields. In terms of boundary-layer theory,[20] the short- and long-wavelength solution can be thought of as the inner and outer solution, respectively. The long-wavelength behavior is obtained by employing a technique initially developed by Suzuki[21] to examine laser models and later extended by Kawasaki, Yalabik, and Gunton[4] to study the time-dependent Ginzburg-Landau equation. This method has recently[22] been applied to a number of different physical systems and has been generalized to a class of dynamical systems. The essence of this method is to resum an infinite singular perturbation series in a late-time long-wavelength limit. This outer solution provides an analytic approximation to the scaling functions and growth exponents for both conserved and nonconserved fields. The short-wavelength behavior is obtained by a technique which is valid once domain walls are well established (i.e., once the ordering field is locally saturated) and for wave vectors of the order of the interfacial width. The inner and outer solution are combined to provide insight into the approach to the scaling regime. In particular, intermediate-time corrections to the growth exponent n, and to Porod's law[23] are explicitly determined.

For a greater understanding of the dynamical system, it is useful to consider a specific example of an ordering process described by model C. Consider a binary alloy (made up of A and B atoms) in which the interaction energy between neighboring atoms favor a state in which all A atoms are surrounded by B atoms (i.e., an AB crystal structure). Examples of experimental systems that have been studied are Cu-Al,[14,24] Fe-Al,[7] and Ti-Al.[11] At low

temperatures these interaction energies cause an ordering of A and B atoms to occur, defining the ordered state. The ordered system contains two sublattices, one on which the A atoms lie and the other on which the B atoms reside. Since the two sublattices are symmetric it is energetically irrelevant to which sublattices the A atoms lie. If c_1 and c_2 are the concentrations of A atoms on sublattices one and two, respectively, then the order parameter (ϕ) describing this system is simply $\phi \equiv (c_1 - c_2)/2$. Thus in an ordered state ϕ is positive if the A atoms are on the first sublattice and negative if they lie on the second. At high temperatures, thermal fluctuations (i.e., entropic influences) dominate and a disordered state arises, which is characterized by $\phi = 0$. The temperature and global concentration of A atoms at which the interaction energies balance the entropic terms is called the c_λ line. When an equilibrated system above this line is quenched below the c_λ line a dynamical ordering process occurs, in which ϕ evolves from 0 to a + or − state. These dynamics are the focus of this work.

Although the field ϕ is globally nonconserved, the dynamics must be coupled to a conserved field, since the total amount of A (or B) atoms is fixed. This field (c) is conveniently described in terms of c_1 and c_2 through the following relationship: $c \equiv (c_1 + c_2)/2$. Thus c denotes the local concentration of A atoms. The free energy ($\mathcal{F}$) of this system can then be expanded in the two fields, i.e.,

$$\mathcal{F} = \int d\mathbf{r} \left[\frac{r}{2}\phi^2 + \frac{u}{4}\phi^4 + \frac{\alpha}{2}\phi^2 c + \frac{w}{2}(c)^2 + \frac{\kappa}{2}|\nabla\phi|^2 \right], \quad (2)$$

where r, u, α, w, and κ are phenomenological temperature-dependent parameters. Odd powers of ϕ do not appear, since the + and − phases are identical. In scattering experiments the structure factor for the ψ field would correspond to the Bragg peak centered at 2π over the lattice constant associated with the ordered AB phase. The structure factor for the c field would correspond to concentration-concentration fluctuations measured at small wave vectors.

The above discussion is also directly applicable to other systems such as an Ising system with antiferromagnetic interactions and Kawasaki dynamics, where, for example, the "A" atoms correspond to "up" spins and the "B" atoms correspond to "down" spins. In addition this free energy has been employed to study isotropic Ising systems on an isotropic compressible lattice,[25] where, the conserved field c is the scalar $\nabla \cdot \mathbf{u}$ and $\mathbf{u}$ is the displacement vector. Bergman and Halperin[25] have shown this free energy to be applicable to compressible liquids, where c is identified with the deviation from the liquid density. Alternatively Eq. (2) has been derived for metamagnets by Nelson and Fisher[26] (which also includes a ϕ^6 term), where ϕ is the sublattice magnetization and c is the magnetization.

Some general comments about the phenomenological parameters can be made. u must be positive, since a negative u would imply unbounded growth of the ϕ field (if u is negative a ϕ^6 term must be included). The coefficient r is positive (i.e., $\mathcal{F}$ has a single well centered at $\phi = 0$) in the disordered state and negative in the ordered phase (i.e., $\mathcal{F}$ has a double-well structure). For the case discussed above, w must also be positive (i.e., the separation of A and B atoms is not energetically favorable). Finally the coupling constant (α) and gradient energy term (κ) are positive. In Appendix A these parameters are determined in terms of microscopic quantities using a Bragg-Williams[7] approximation for the free energy. An important feature of this model is the existence of a tricritical point. This point is defined by the temperature and global concentration at which the c_λ line coincides with $\partial^2\mathcal{F}/\partial c^2 = 0$. From Eq. (2) this occurs when $(r + \alpha c) = 0$ and $\alpha^2/(2uw) = 1$. Below the tricritical point phase separation in the c field occurs even for positive w. In this paper, the dynamics will be studied above the tricritical point, but below the c_λ line (i.e., $\alpha^2/(2wu) < 1$ and $r < 0$).

The dynamics of the disorder-order transition involve the growth of positive and negative domains (in ϕ) separated by antiphase boundaries. As discussed above, it has long been accepted that these domains grow as a power law in time and the correlations of ϕ should scale in time. A great deal of progress has been made for $\alpha = 0$. In this case the two fields are completely decoupled and the dynamics are described by model A.[2] Allen and Cahn[7(c)] have presented a theory for the dynamics of antiphase boundaries, while, Ohta, Jasnow, and Kawasaki[6] and Kawasaki, Yalabik, and Gunton[4] have obtained approximate solutions to model A in the late-time long-wavelength limit. Although the method for obtaining these solutions is different, the solutions themselves are identical. The result of these works is the prediction for the two-point correlation function ($\langle \phi(\mathbf{r}_1, t)\phi(\mathbf{r}_2, t) \rangle$) and $n = \frac{1}{2}$. These predictions compare favorably with numerical simulations of various nonconserved systems, such as model A,[8] an Ising system with long- (but finite-) range interactions[15] and the Potts model on a triangular lattice.[13] For sufficiently long times, the softness of the domain walls should be irrelevant, since the domain size D becomes arbitrarily large. Nevertheless there can be important crossover effects for early to intermediate times. The main discrepancy in these approximations is that they contain infinitely sharp domain walls, while the real systems have soft domain walls. Recently Mazenko, Valls, and Zannetti[27] have developed an ambitious theory for domain growth in both models A and B. In addition Oono and Puri[8] have determined the first-order corrections to Porod's law due to soft domain walls. Numerically Sahni *et al.*[28] have conducted a Monte Carlo study of a tricritical system.

The more interesting problem of a nonzero α has been considered by Zia *et al.*[5] and Mullins and Viñals.[9] The work of Zia *et al.*[5] examines the stability of a planar interface to infinitesimal perturbations. The linear dispersion relationship obtained in this work implies that perturbations in the interface decay like $k^2 t$ for $\langle \phi \rangle = 0$ and $k^3 t$ for $\langle \phi \rangle \neq 0$. From this a growth exponent of $\frac{1}{2}$ in the former case and $\frac{1}{3}$ in the latter can be inferred. By assuming self-similarity Mullins and Viñals[9] predict a growth exponent of $\frac{1}{2}$ for the $\langle \phi \rangle = 0$ case. These predictions will be examined in the following pages.

The structure of the paper is as follows. In the next

section the dynamical equations for model C are presented and expressed in dimensionless form. Following this section a linear-stability analysis of these equations is derived. An asymptotic analysis of both the long and short wavelengths is presented in Secs. IV and V. The two asymptotic solutions are then combined to obtain a late-time solution for all wavelengths. The asymptotic solutions are used to determine the scaling function for the correlation functions of the two fields and the dynamic growth exponents in Secs. VII and VIII. In the succeeding section early-time correction due to the interfacial width are determined from the asymptotic solutions. Finally, a summary of the findings is presented.

II. DYNAMICAL EQUATIONS

The time derivatives of the conserved and nonconserved fields are proportional to the functional derivative of the free energy with respect to c and ϕ, respectively. To maintain the global conservation law for c, the functional derivative is multiplied by a Laplacian. In the absence of thermal noise, the dynamical system is described by the following equations:

$$\frac{\partial \phi}{\partial t} = -\Gamma_\phi \frac{\delta \mathcal{F}}{\delta \phi} , \tag{3}$$

$$\frac{\partial c}{\partial t} = \Gamma_c \nabla^2 \frac{\delta \mathcal{F}}{\delta c} , \tag{4}$$

where Γ_ϕ and Γ_c are phenomenological constants. Assuming r is negative and the other phenomenological parameters in Eq. (2) are positive, these equations can be transformed into a dimensionless form, using

$$\mathbf{x} = (|r|/\kappa)^{1/2}\mathbf{r} , \tag{5}$$

$$\psi = (u/|r|)^{1/2}\phi , \tag{6}$$

$$\tau = (\Gamma_\phi |r|)t , \tag{7}$$

$$h = (\alpha/|r|)c . \tag{8}$$

In these variables the dynamical equations of motion for the two dimensionless fields (ψ and h) become

$$\frac{\partial \psi}{\partial \tau} = (1+\nabla^2)\psi - \psi^3 - \psi h \tag{9}$$

and

$$\frac{\partial h}{\partial \tau} = R\nabla^2(h + \alpha'\psi^2) , \tag{10}$$

where

$$R = \left[\frac{\Gamma_c}{\Gamma_\psi}\right]\left[\frac{w}{\kappa}\right] \tag{11}$$

and

$$\alpha' = \alpha^2/(2wu) . \tag{12}$$

Thus, there are only two parameters in the dimensionless equations of motion, namely R and α'. The parameter R is the product of the ratios of the respective time and length scales of the two fields, while α' controls the strength of the coupling between the two fields. In these units the tricritical point is defined by $\alpha' = 1$ and $h = 1$. To estimate the magnitude of the coupling constant, a Bragg-Williams approximation for $\mathcal{F}$ will be employed with the addition of an elastic energy term (see Ref. 7 and Appendix A). In Fig. 1 α' is plotted as a function of concentration at a temperature (i.e., $T = 1000$ K) above the tricritical point for the Fe-Al system. The coupling disappears at perfect stoichiometry (i.e., $c_0 = 0.5$) for zero elastic energy and increases symmetrically about $c_0 = 0.5$. Thus, the conserved field is only important when the mean concentration does not match the concentration of the preferred crystal structure, unless elastic energies deform the antiphase boundaries. The growth of a crystal phase for $\alpha' < 1$ will be considered in this work. In the following section a linear-stability analysis of the coupled dynamical system described by Eqs. (9) and (10) will be presented.

III. LINEAR STABILITY ANALYSIS

The model system discussed in the preceding section will now be analyzed by linearizing about the average value of both fields, where $\delta\psi$ and δh are defined to be fluctuations about the average value of ψ and h, respectively:

$$\psi \equiv \psi_0 + \delta\psi \tag{13}$$

and

$$h \equiv h_0 + \delta h . \tag{14}$$

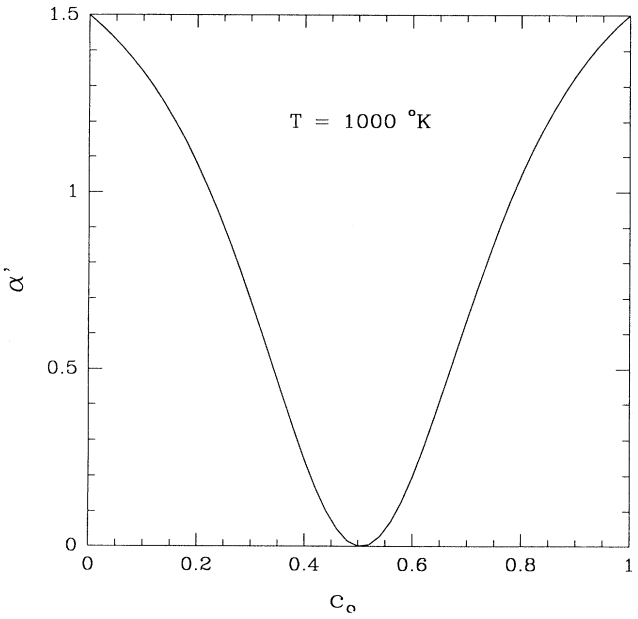

FIG. 1. Coupling constant (α') evaluated for an Fe-Al system through Eq. (A2) as a function of average concentration. In this figure, $T = 1000$ K, $Y' = 463$ K/T, $V_1' + V_2' = 175$ K/T, $e_c = 0.45$, and $e_\phi = -0.22$. These values were taken from Ref. 7(a).

The ordering process described in the Introduction was for $\psi_0=0$, in which there is an equal amount of A atoms on each sublattice. As time evolves this condition is violated locally as domains are formed, but is maintained globally. Substituting Eqs. (13) and (14) into Eqs. (3) and (4) and retaining terms to first order in $\delta\psi$ and δh, the linearized equations of motion in Fourier space are

$$\frac{\partial}{\partial\tau}\delta\psi(\mathbf{q},\tau)=\gamma_q\delta\psi(\mathbf{q},\tau)-\psi_0\delta h(\mathbf{q}\tau) \tag{15}$$

and

$$\frac{\partial}{\partial\tau}\delta h(\mathbf{q},\tau)=-\beta_q\delta h(\mathbf{q},\tau)-2\alpha'\psi_0\beta_q\delta\psi(\mathbf{q},\tau)\ . \tag{16}$$

The various quantities in these equations are

$$\gamma_q\equiv 1-3\psi_0^2-h_0-q^2\ , \tag{17}$$

$$\beta_q\equiv Rq^2\ , \tag{18}$$

$$\delta\psi(\mathbf{q},\tau)\equiv\int d\mathbf{x}\,e^{i\mathbf{q}\cdot\mathbf{x}}\delta\psi(\mathbf{x},\tau)\ , \tag{19}$$

and

$$\delta h(\mathbf{q},\tau)\equiv\int d\mathbf{x}\,e^{i\mathbf{q}\cdot\mathbf{x}}\delta h(\mathbf{x},\tau)\ . \tag{20}$$

Equation (15) indicates that ψ_0 plays the role of an external field. For the binary alloy system, a positive ψ_0 makes sublattice 1 energetically favorable for the A atoms to reside. Although this situation is unlikely to occur in the binary system described earlier, it may be of interest in some other systems (such as in solidification problems where the latent heat created in the freezing or melting transition couples like a field). The dynamics for $\psi_0\neq 0$ are significantly different from the $\psi_0=0$ case. The reason for this can be seen by examining the free energy. For $\psi_0=0$, $\mathcal{F}$ is minimized when $h=0$ in the bulk ψ phases, and consequently h does not separate into two domains. In contrast, when $\psi_0\neq 0$, $\mathcal{F}$ contains a term proportional to $\delta\psi\delta h$, and is minimized when $\delta h\propto-\delta\psi$. Since δh is a conserved field that must itself separate, the dynamics are considerably altered. For systems controlled by a conserved variable the dynamics should lead to a growth exponent of $\frac{1}{3}$. This is consistent with the work of Zia *et al*,[5] which predicts that fluctuations about planar interfaces decay as q^3t. The late-stage dynamics of a conserved field is much more difficult to study, due to nonlocal interface interactions. This case will not be considered in the following sections, but will be discussed in the succeeding linear analysis.

The linearized solution provides some insight into the influence of ψ_0 on the dynamical behavior of this system. The eigenvalues ($\lambda_\pm$) of Eqs. (15) and (16) are

$$\lambda_\pm(q)=\frac{\gamma_q-\beta_q\pm\sqrt{(\gamma_q+\beta_q)^2+8\alpha'\psi_0^2\beta_q}}{2}\ . \tag{21}$$

The negative eigenvalue (i.e., λ_-) is always less than or equal to zero (zero at $q=0$), and hence corresponds to linearly stable growth. This can be seen by noting that $\gamma_q-\beta_q\leq\gamma_q+\beta_q$, which implies that

$$\gamma_q-\beta_q\leq\sqrt{(\gamma_q+\beta_q)^2+8\alpha'\psi_0^2\beta_q}\ .$$

In contrast, the positive eigenvalue is always greater than zero, if $3\psi_0^2+h_0<1$. To further illuminate this point it is useful to consider λ_+ in the long-wavelength limit, i.e.,

$$2\lambda_+\approx(1-3\psi_0^2-h_0)-q^2\left[1-\frac{2R\alpha'\psi_0^2}{1-3\psi_0^2-h_0}\right]+\cdots\ . \tag{22}$$

When $1-3\psi_0^2-h_0>0$ the system is linearly unstable. The limit of linear instability is used to define the classical spinodal which roughly delineates nucleation from spinodal decomposition. Thus the classical spinodal is defined by $3\psi_0^2+h_0=1$. It is interesting to note that λ_+ is maximized at $q=0$ when $1-3\psi_0^2-h_0>2R\alpha'\psi_0^2$ and at $q>0$ for $1-3\psi_0^2-h_0<2R\alpha'\psi_0^2$. Thus in this linear analysis the dominant length scale will be infinite for the former case and finite in the latter. In Fig. 2 this feature is illustrated by plotting the wave vector $q_{\max}$, at which λ_+ peaks as a function of R for $h_0=0$ and $\psi_0=0.2$, 0.3, 0.4, and 0.5. In nonconserved systems the peak in the structure factor always occurs at $q=0$ and leads toward a growth exponent of $n=\frac{1}{2}$. In conserved systems the peak in the linear solution is at a nonzero wave vector and the growth exponent is $\frac{1}{3}$. Thus it may be of some interest to examine the process when $\psi_0\neq 0$, but $1-3\psi_0^2-h_0>2R\alpha'\psi_0^2$.

The linear solution is particularly simple when $\psi_0=0$, i.e.,

$$\delta\psi(\mathbf{q},\tau)=e^{\gamma_q\tau}\delta\psi(\mathbf{q},0) \tag{23}$$

and

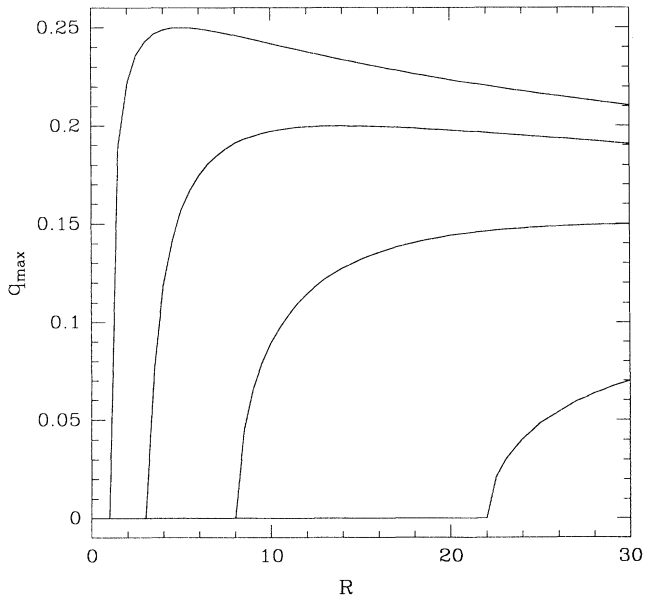

FIG. 2. Dependence of maximum of linear dispersion relation given in Eq. (21) (for λ_+) on the ratio (R) of length and time scales of two fields. The lines from left to right correspond to $\psi_0=0.2$, 0.3, 0.4, and 0.5, for $h_0=0$.

$$\delta h(\mathbf{q},\tau)=e^{-\beta_q\tau}\delta h(\mathbf{q},0)\ . \tag{24}$$

Thus the two linear solutions completely decouple. The ψ field in this approximation grows exponentially in time and the h field decays to zero exponentially. The unbounded growth of ψ predicted in this analysis is clearly in contradiction of the physical picture in which ψ saturates at finite values. The saturation of ψ is taken into account by the nonlinear terms as will be shown in the nonlinear analysis of the following sections.

In the preceding analysis the solution is linearized around the initial average values of the two fields. If the fields are linearized around the two phase states, quite a different result occurs. This approach has been employed by San Miguel[29] *et al.* in tricritical systems. One result of this analysis is the prediction of another classical spinodal at $\alpha'=1$. As discussed in the Introduction the temperature and average concentration at which this spinodal coincides with the other spinodal (i.e., $3\psi_0^2+h_0=1$) defines the tricritical point. Both these "spinodals" arise naturally in the analysis of the stationary solution of the short-wavelength modes as discussed in Sec. V.

IV. LONG-WAVELENGTH SOLUTION (OUTER SOLUTION)

In this section an asymptotic solution to the coupled dynamical system will be presented for $\psi_0=0$. As discussed in the Introduction this corresponds to the order-disorder transition in binary alloys across the c_λ line. In the following derivation an approximate form for both the ψ and h field will be obtained. The first step in this derivation is to rewrite Eqs. (9) and (10) in integral form, so that a diagrammatic expansion can be developed. The integral representation is

$$\psi(\mathbf{q},\tau)=\psi^0(\mathbf{q},\tau)-\int_0^\tau d\tau' e^{\gamma_q(\tau-\tau')}\int d\mathbf{x}\, e^{i\mathbf{q}\cdot\mathbf{x}}[\psi^3(\mathbf{x},\tau)+\psi(\mathbf{x},\tau)\delta h(\mathbf{x},\tau)]\ , \tag{25}$$

$$\delta h(\mathbf{x},\tau)=\delta h^0(\mathbf{x},\tau)-\alpha'\beta_q\int_0^\tau d\tau' e^{-\beta_q(\tau-\tau')}\psi^2(\mathbf{x},\tau')\ , \tag{26}$$

where $\psi^0(\mathbf{x},\tau)\equiv e^{\gamma\tau}\psi(\mathbf{x},0)$ and $\delta h^0(\mathbf{x},\tau)\equiv e^{-\beta\tau}\delta h(\mathbf{x},0)$. In this analysis $\psi_0=0$, and thus $\delta\psi=\psi$. For simplicity the initial fluctuations in h will be set to zero. This restriction is not very important, since $\delta h^0(\mathbf{x},\tau)$ goes to zero in the asymptotic limit. An equation for ψ can be written in closed form, since the right-hand side of Eq. (26) does not depend on $\delta h(\mathbf{x},\tau)$, i.e.,

$$\psi(\mathbf{x},\tau)=\psi^0(\mathbf{x},\tau)-\int_0^\tau d\tau' e^{\gamma_q(\tau-\tau')}\int d\mathbf{x}\, e^{i\mathbf{q}\cdot\mathbf{x}}\psi^3(\mathbf{x},\tau')+\alpha'\int_0^\tau d\tau' e^{\gamma_q(\tau-\tau')}\int_0^{\tau'} d\tau''\int d\mathbf{x}\, e^{i\mathbf{q}\cdot\mathbf{x}}\psi(\mathbf{x},\tau')\beta e^{-\beta(\tau'-\tau'')}\psi^2(\mathbf{x},\tau'')\ . \tag{27}$$

A diagrammatic expansion of eq. (27) is given in Fig. 3. In this figure the solid lines terminating in a circle represent the vertex,

$$\int_0^\tau d\tau' e^{\gamma_q(\tau-\tau')}\int d\mathbf{x}\, e^{i\mathbf{q}\cdot\mathbf{x}}$$

and the solid lines terminating in a diamond represent the vertex,

$$\alpha'\int d\mathbf{k}_1 d\mathbf{k}_2 d\mathbf{k}_3\delta(\mathbf{q}-\mathbf{k}_1-\mathbf{k}_2-\mathbf{k}_3)\int_0^\tau d\tau' e^{\gamma_q(\tau-\tau')}\int_0^{\tau'} d\tau'' e^{-\beta_{\mathbf{k}_1+\mathbf{k}_2}(\tau'-\tau'')}\beta_{\mathbf{k}_1+\mathbf{k}_2}\ .$$

The second time integral in this vertex (i.e., over τ'') operates only on lines emerging in from the top and bottom corners of the diamond. The solid lines represent the bare propagator or linear solution for the ψ field [i.e., $\psi^0(\mathbf{x},\tau)$].

A general diagram in this expansion can be significantly simplified in the late-time long-wavelength limit, by considering the similar features of each diagram. If n equals the number of circle vertices and m equals the number of diamond vertices in a given diagram, then there are $n+2m$ time integrals and $2(m+n)+1$ wave-vector integrals (once all δ functions are integrated out). The integrand of these space and time integrals will contain a product of $n+m$ functions of the form $e^{\gamma_{\mathbf{k}_i}\tau_j}$ and m products of functions of the form $e^{-\beta_{\mathbf{k}_i}\tau_j}$ (where k_i and τ_j are integration variables or sums of integration variables). The time integrals can be evaluated in the asymptotic limit by assuming that $e^{\gamma_q\tau}$ is much greater than one

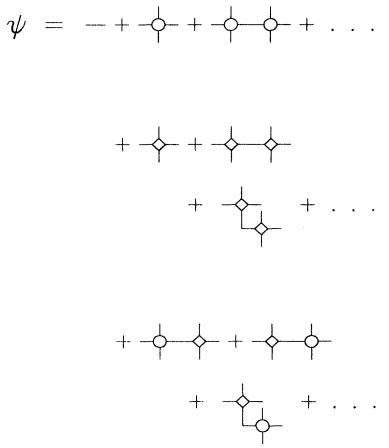

FIG. 3. Diagrammatic expansion of ψ field [i.e., Eq. (27)]. The relationship between the symbols and their mathematical counterparts is given in the text.

near $q=0$. Once the time integrals have been performed the resultant diagram will contain Fourier integrals over products of $e^{\gamma_{\mathbf{k}_i}\tau}$ and $e^{-\beta_{\mathbf{k}_j}\tau}$, leading to integrals of the form

$$\int d\mathbf{k}_1 d\mathbf{k}_2 \cdots \exp[(\gamma_{k_1}+\gamma_{k_2}+\cdots-\beta_{k_i}+\cdots)\tau] \; G(\mathbf{k}_1,\mathbf{k}_2,\ldots) ,$$

where G is dependent on the specific diagram. In the limit that $\tau\to\infty$ the integrals can be approximated by Laplace's integral approximation[20] since the maximum of $(\gamma_{k_1}+\gamma_{k_2}+\cdots-\beta_{k_i}+\cdots)$ is greater than zero. For illustrative purposes a typical integral is approximated below:

$$\begin{aligned}\int d\mathbf{k}_i \int_0^{\tau_{j-1}} d\tau_j e^{\gamma_{\mathbf{k}_i}\tau_j} G(\mathbf{k}_i)\psi(\mathbf{k}_i,0) &= \int d\mathbf{k}_i \frac{(e^{\gamma_{\mathbf{k}_i}\tau_{j-1}}-1)}{\gamma_{\mathbf{k}_i}} G(\mathbf{k}_i)\psi(\mathbf{k}_i,0) \\ &\approx \frac{G(0)}{\gamma_{\mathbf{k}_{i=0}}} \int d\mathbf{k}_i e^{\gamma_{\mathbf{k}_i}\tau_{j-1}} \psi(\mathbf{k}_i,0) . \qquad (28)\end{aligned}$$

This approximation asserts that G can be expanded about the maximum of exponential (i.e., at $k_i=0$). To first order, all diagrams containing a diamond vertex are asymptotically zero, since G will be a product that contains at least one β which is zero at $k_i=0$. Thus all diagrams containing a diamond vertex are zero. In simple terms, diagrams that are proportional to β are zero in the long-wavelength late-time limit.

The above approximations imply the $\delta h(\mathbf{x},\tau)$ field is slaved to the ψ field. Thus the equation of motion for ψ is identical to that for the time-dependent Ginzburg-Landau equation for a nonconserved order parameter (i.e., model A). An asymptotic summation of this series was presented by Kawasaki, Yalabik, and Gunton.[4] The technique for evaluating the nonvanishing diagrams is the same as discussed in the above paragraph. Once the late-time long-wavelength approximation has been made the series can be resummed. The approximate late-time long-wavelength solution for the ψ field is then

$$\psi(\mathbf{x},\tau)\approx \frac{\psi^0(\mathbf{x},\tau)}{\{1+[\psi^0(\mathbf{x},\tau)/A]^2\}^{1/2}} \approx A\frac{\psi^0(\mathbf{x},\tau)}{|\psi^0(\mathbf{x},\tau)|} , \qquad (29)$$

where $A\equiv(1-h_0)^{1/2}$, and the second equivalence occurs at very late times. Since $\psi^0(\mathbf{x},\tau)$ grows exponential in time this solution quickly saturates to $\pm(1-h_0)^{1/2}$ in the bulk with very sharp domain walls separating the phases. The prediction of infinitely sharp walls separating the domains does not agree with the well-known hyperbolic tangent profile solution of the stationary one-dimensional problem. This discrepancy is a direct consequence of the large wavelength approximation used in summing the diagrammatic series. In the next section a technique for obtaining the short-wavelength behavior of ψ will be presented and combined with Eq. (29).

Equation (29) predicts that the interfacial position is completely described by the zeros of the linear solution. Consequently the interface is Gaussianly correlated (since the linear solution itself is Gaussianly correlated). Clearly this method cannot be applied to conserved systems where very strong nonlocal interactions dominate the interface dynamics. The position of the interfaces in this approximation is identical to that obtained by Ohta, Jasnow, and Kawasaki[6] using an interfacial dynamics method.

To evaluate the $\delta h(\mathbf{x},\tau)$ field it is convenient to consider Eq. (26) with the variable change $v=\tau'/\tau$, i.e.,

$$\delta h(\mathbf{q},\tau)=\alpha'\beta_q e^{\beta_q\tau}\tau\int_0^1 dv\, e^{(-\beta_q\tau)v}\int d\mathbf{x}\, e^{i\mathbf{q}\cdot\mathbf{x}}\psi^2(\mathbf{x},v\tau) . \qquad (30)$$

The integral can be asymptotically evaluated using Laplace's integral approximation in the limit $-\beta_q\tau\gg1$. In this limit, $e^{(-\beta_q\tau)v}$ is a maximum in the interval $\{0,1\}$ at $v=1$. Equation (30) can then be expanded in the following fashion:

$$\delta h(\mathbf{q},\tau)=\alpha'\beta_q e^{\beta_q\tau}\tau\int_0^1 dv\, e^{(-\beta_q\tau)v}\left[\int d\mathbf{x}\, e^{i\mathbf{q}\cdot\mathbf{x}}\psi^2(\mathbf{x},v\tau)\Big|_{v=1}+\left[\frac{\delta}{\delta v}\int d\mathbf{x}\, e^{i\mathbf{q}\cdot\mathbf{x}}\psi^2(\mathbf{x},v\tau)\right]\Big|_{v=1}(v-1)+\cdots\right] . \qquad (31)$$

Retaining the first term in this expansion leads to the following approximation of $\delta h(\mathbf{x},\tau)$:

$$\delta h(\mathbf{q},\tau)\approx\alpha'(e^{\beta_q\tau}-1)\int d\mathbf{x}\, e^{i\mathbf{q}\cdot\mathbf{x}}\psi^2(\mathbf{x},\tau) . \qquad (32)$$

The next-order correction term is of the order $\tau e^{-2(1-h_0)\tau}$ (see Appendix B). It should be noted that this formula can be easily modified to include higher-order terms in the gradient expansion for h in the free energy provided these terms do not create a linear instability in h. For example, if a term proportional to $|\nabla h|^2$ appeared in the free energy, then the relaxation term would become

$$(e^{-\beta_q\tau}-1)\to\left[\frac{e^{-\beta'_q\tau}-1}{1+q^2}\right] , \qquad (33)$$

where $\beta'_q\equiv Rq^2(1+q^2)$.

Although Eq. (32) was derived for $\delta h(\mathbf{x},\tau)$ in the limit

$\beta_q\tau \gg 1$, it still maintains the conservation law, since for small q, $e^{-\beta_q\tau}-1 \approx -Rq^2\tau$. This equation combined with Eq. (29) provides a description of the dynamics in the limit of vanishing domain-wall width. Since $\delta h(\mathbf{x},\tau)$ is zero everywhere except at domain walls, it is important to incorporate a finite domain-wall thickness, ideally in terms of the proper hyperbolic tangent profile. In the next section an approximation for the short-wavelength fluctuations (or interfacial profile) of ψ is made and in Sec. VII it is incorporated with the long-wavelength approximation.

V. SHORT-WAVELENGTH SOLUTION (INNER SOLUTION)

The interfacial profile of the ψ field can be obtained by considering the short-wavelength behavior in the asymptotic limit. Since the width of the interface is a nonscaling length it reaches its asymptotic value very quickly compared with the slow power-law growth of the domains. To obtain this short-wavelength behavior it is convenient to make the substitution $v=\tau'/\tau$ in Eq. (25), i.e.,

$$\psi(\mathbf{q},\tau)=\psi^0(\mathbf{q},\tau)-\tau e^{\gamma_q\tau}\int_0^1 dv\, e^{(-\gamma_q\tau)v}\int d\mathbf{x}\, e^{i\mathbf{q}\cdot\mathbf{x}}[\psi^3(\mathbf{x},v\tau)+\delta h(\mathbf{x},v\tau)\psi(\mathbf{x},v\tau)] \ . \tag{34}$$

In the late-time short-wavelength limit [i.e., $-\gamma_q\tau \gg 1$, or $(q^2-1+h_0)\tau \gg 1$] the integrand can be expanded around the maximum of v in the interval $\{0,1\}$. Retaining the first term in the expansion gives

$$\psi(\mathbf{q},\tau)\approx\psi^0(\mathbf{q},\tau)+\frac{1}{\gamma_q}(1-e^{\gamma_q\tau})\int d\mathbf{x}\, e^{i\mathbf{q}\cdot\mathbf{x}}[\psi^3(\mathbf{x},\tau)+\delta h(\mathbf{x},\tau)\psi(\mathbf{x},\tau)] \ . \tag{35}$$

In the asymptotic short-wavelength limit $e^{\gamma_q\tau}$ can be set to zero. In this limit Eq. (32) becomes

$$\delta h(\mathbf{x},\tau)\approx\alpha'[\langle\psi^2\rangle-\psi^2(\mathbf{x},\tau)] \ , \tag{36}$$

which can be further simplified by noting that $\langle\psi^2\rangle\rightarrow 1-h_0$. Substituting this expression for $\delta h(\mathbf{x},\tau)$ into Eq. (35) and setting $e^{\gamma_q\tau}=0$ gives the following result:

$$\nabla^2\psi=(1-\alpha')[\psi^3-\psi(1-h_0)] \ . \tag{37}$$

The one-dimensional solution of this equation is well known [for fixed boundary conditions, i.e., $\psi(x\rightarrow-\infty)\rightarrow -A$ and $\psi(x\rightarrow+\infty)\rightarrow +A$] and is

$$\psi(x)=A\tanh(x/W) \ , \tag{38}$$

where

$$W\equiv\left[\frac{2}{(1-h_0)(1-\alpha')}\right]^{1/2} \ . \tag{39}$$

As h_0 or α' approaches 1 the interfacial width diverges. Consequently this analysis predicts interesting behavior at $h_0=1$ and $\alpha'=1$, which is, of course, the tricritical point.

Equation (29) together with this result describe the influence of the conserved field on the dynamics of the ordering field. The rate of growth of domains is unaffected by h_0, since the zeros of the linear solution are independent of h_0. In contrast the amplitude of ψ and interfacial width are altered through Eqs. (39) and (29). Although W does not influence the asymptotic scaling form it can play an important role in the approach to scaling. In the next section the short- and long-wavelength solutions will be combined.

VI. SOFT WALL SOLUTION

In the preceding sections both the long-and short-wavelength behavior of the dynamical system were approximated in the asymptotic time limit. The critical difference between the two solutions is the time scales on which the dynamics evolve. In essence the interface motion described by the zeros of Eq. (29) evolve in a power-law fashion. In contrast, the shape of the domain walls equilibrate to their final shape exponentially in time. Consequently the shape of the walls is frozen long before the process of phase separation is completed, which implies that the two dynamics are decoupled in the late-time limit (in this context "late" time means $e^{R\tau}\gg 1$ and $e^{(1-h_0)\tau}\gg 1$). In this section , the decoupling is used to construct an approximation for ψ that includes both the long- and short-wavelength fluctuations.

To accomplish this task, it is assumed that the domains are large enough that ψ has reached its maximum amplitude (i.e., A) in the center of each domain. As discussed previously, the separation of time scales allows one to write the soft (i.e., the one consistent with a hyperbolic tangent) solution $[\psi^{\text{soft}}(\mathbf{x},\tau)]$ as a convolution of some shaping function ($\mathcal{S}$) with the sharp or hard wall $[\psi^{\text{hard}}(\mathbf{x},\tau)]$ solution. The shaping function can be obtained by considering a hard solution that is $-A$ from $x=-\infty$ to $x=0$ and $+A$ from $x=0$ to $x=\infty$, and requiring

$$\int_{-\infty}^{\infty}\mathcal{S}(x+x')\psi^{\text{hard}}(x')=A\tanh(x/W) \ . \tag{40}$$

By substitution it is easy to show that

$$\mathcal{S}(x)=-\frac{\operatorname{sech}^2(x/W)}{2W} \tag{41}$$

satisfies this equation. Thus in Fourier space the full soft wall solution for ψ can be written

$$\psi^{\text{soft}}(\mathbf{q},\tau)=\mathcal{S}(qW)\psi^{\text{hard}}(\mathbf{q},\tau) \ , \tag{42}$$

where

$$\mathcal{S}(qW)\equiv\left[\frac{q\pi W}{2}\right]\operatorname{csch}\left[\frac{q\pi W}{2}\right] \tag{43}$$

and

$$\psi^{\text{hard}}(\mathbf{x},\tau) \equiv A \frac{\psi^0(\mathbf{x},\tau)}{|\psi^0(\mathbf{x},\tau)|} \ . \tag{44}$$

Equation (42) can then be substituted into Eq. (32) to obtain a soft solution for $\delta h(\mathbf{x},\tau)$. A more convenient way to obtain a soft solution for $\delta h(\mathbf{x},\tau)$ is to express $\delta h(\mathbf{x},\tau)$ in terms of a convolution over the zeros of the linear solution with another shaping function. This unknown function is again chosen to be consistent with the hyperbolic profile of the ψ solution. The soft ψ^2 can be written

$$[\psi^{\text{soft}}(\mathbf{x},\tau)]^2 = A^2 \left\{ -\sum_i \left[1 - \tanh^2 \left[\frac{(\mathbf{x}-\mathbf{x}_i)}{W} \right] \right] + 1 \right\} , \tag{45}$$

where the $\mathbf{x}_i$ represents the zeros of the linear solution. This can be further rewritten

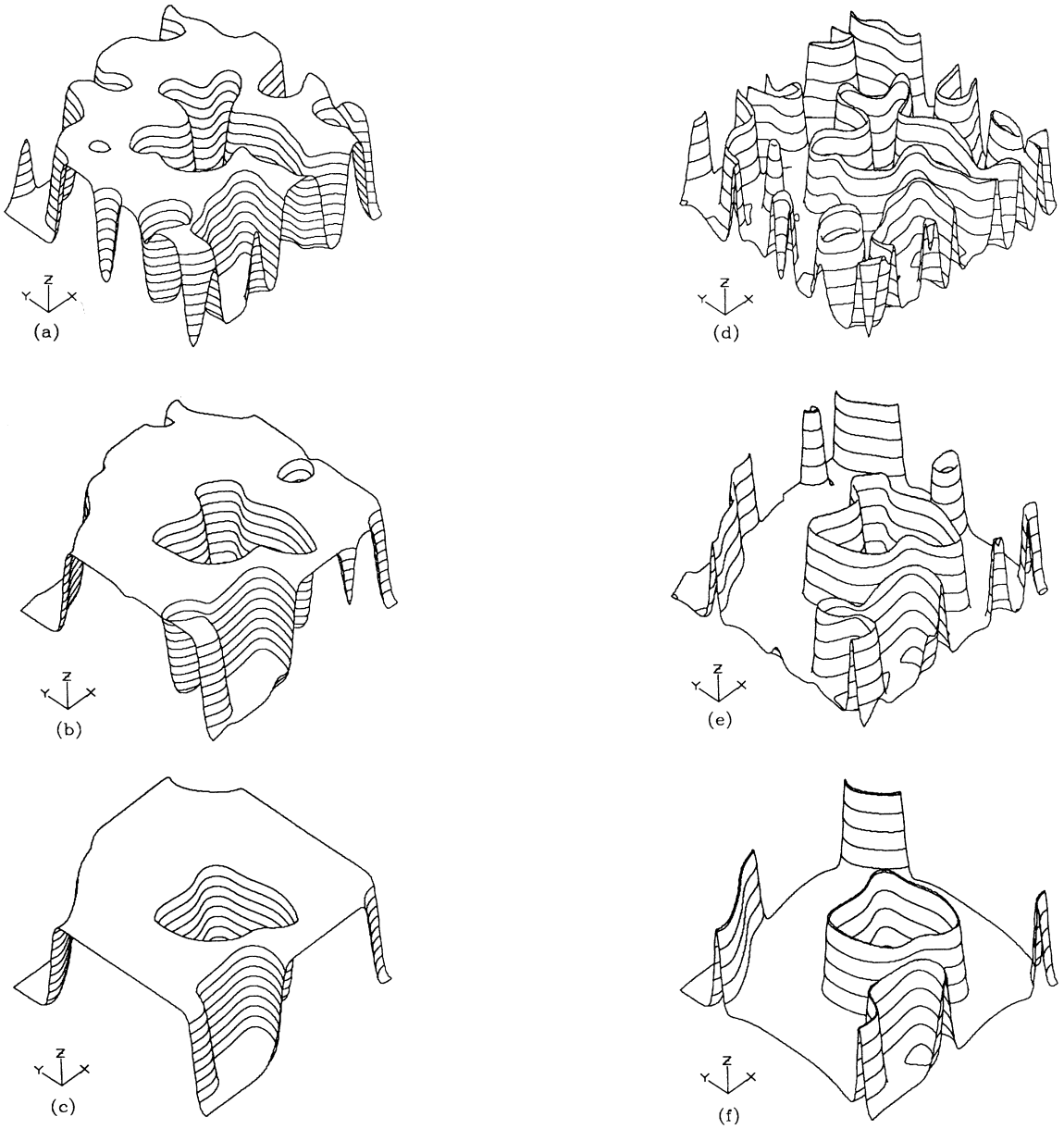

FIG. 4. Three-dimensional representation of soft wall solution for both nonconserved [Figs. 4(a)–4(c)] and conserved [Figs. 4(d)–4(f)] fields, as constructed through Eqs. (42) and (50), respectively for a random initial condition for ψ and for $\alpha' = 0.5$, $h_0 = 0$, and $R = 1$. (a) and (d) are at $\tau = 30$, (b) and (e) are at $\tau = 60$, and (c) and (f) are at $\tau = 90$. In all figures the x and y axes are spatial coordinates and the z axes are ψ and δh in (a)–(c) and (d)–(f), respectively.

$$[\psi^{\text{soft}}(\mathbf{x},\tau)]^2 = A^2\left[-\int d\mathbf{x}' p(\mathbf{x}',\tau)\,\text{sech}^2\left[\frac{(\mathbf{x}-\mathbf{x}')}{W}\right]+1\right], \tag{46}$$

where p describes the interface position, i.e.,

$$p(\mathbf{x},\tau) = \sum_i \delta(\mathbf{x}-\mathbf{x}_i(\tau)) . \tag{47}$$

In Fourier space, Eq. (46) becomes

$$\int d\mathbf{x}\, e^{i\mathbf{q}\cdot\mathbf{x}}[\psi^{\text{soft}}(\mathbf{x},\tau)]^2 = A^2\left[q\pi W^2 \text{csch}\left[\frac{q\pi W}{2}\right]\int d\mathbf{x}\, e^{i\mathbf{q}\cdot\mathbf{x}} p(\mathbf{x},\tau)+\delta(\mathbf{q})\right] . \tag{48}$$

By definition

$$p(\mathbf{x},\tau) = |\nabla\psi^0(\mathbf{x},\tau)|\delta(\psi^0(\mathbf{x},\tau)) . \tag{49}$$

Thus, $\delta h(\mathbf{q},\tau)$ becomes

$$\delta h^{\text{soft}}(\mathbf{q},\tau) = \alpha'(e^{\beta_q \tau}-1)2WA^2\mathcal{S}(qW)\int d\mathbf{x}\, e^{i\mathbf{q}\cdot\mathbf{x}}|\nabla\psi^0(\mathbf{x},\tau)|\delta(\psi^0(\mathbf{x},\tau)) . \tag{50}$$

The physical interpretation of this equation is quite simple. The first term (α') is the coupling constant. The second piece $|e^{\beta_q \tau}-1|$ gives the relaxation to equilibrium, and the third piece $[2WA^2\mathcal{S}(qW)]$ describes the interfacial shape (or goldstone boson). The last term is simply the interface position.

Equations (42) and (50) are the main results of this paper. They give an approximate solution to the asymptotic behavior of the fields $\delta h(\mathbf{x},\tau)$ and ψ. To illustrate the influence of the shaping function on the two fields a three-dimensional plot of these two fields is displayed in Figs. 4 at $\tau=30$, 60, and 90. These figures were obtained by dynamically evolving a random initial configuration for ψ^{hard} according to Eq. (44). This result was then substituted into Eqs. (42) and (50) to obtain a soft solution for ψ and $\delta h(\mathbf{x},\tau)$ for the parameters $\alpha'=0.5$, $h_0=0$, and $R=1$. These figures indicate that the h field is relatively constant except at the interfaces. To examine the interfacial structure a cross section of these configurations is plotted in Fig. 5, in which both fields are plotted versus x position for one value of y. This figure shows the shape of the $\delta h(\mathbf{x},\tau)$ field near interfaces. The value of $\delta h(\mathbf{x},\tau)$ in the bulk domains is slightly negative, to offset the positive values near interfaces [i.e., the conservation law requires that $\langle \delta h(\mathbf{x},\tau)\rangle = 0$]. In the following section the asymptotic solutions will be used to obtain the correlation functions for the two fields.

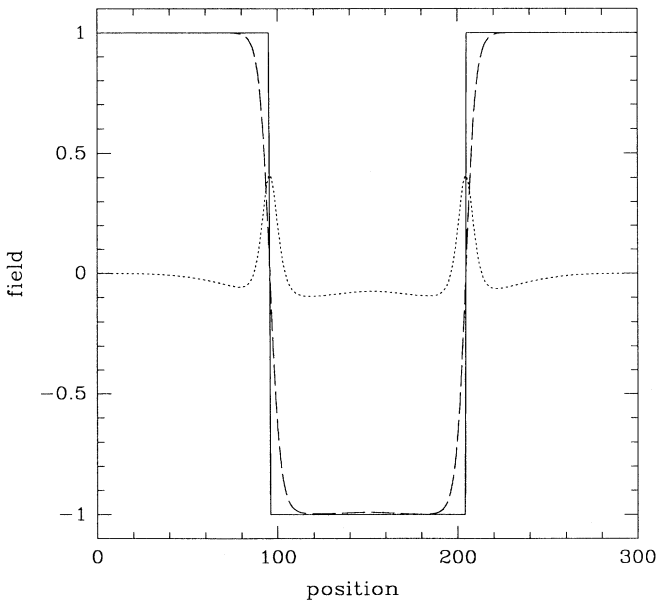

FIG. 5. Cross section of Figs. 4(c) and 4(f). The dashed and dotted lines correspond to the ψ and δh fields, respectively. The solid line is ψ^{hard}.

VII. CORRELATION FUNCTIONS

The correlation of the nonconserved field can easily be determined since the interface shape function does not affect the correlations of the domains. The two-point correlation function,

$$S_\psi(q,\tau) = \langle \psi(\mathbf{q},\tau)\psi(-\mathbf{q},\tau)\rangle ,$$

can be approximated using Eq. (42), i.e.,

$$S_\psi(q,\tau) \approx \mathcal{S}^2(qW)\langle \psi^{\text{hard}}(\mathbf{q},\tau)\psi^{\text{hard}}(-\mathbf{q},\tau)\rangle . \tag{51}$$

The correlation function in the above equation has been determined by many authors using various methods.[3,4,6] Using this standard result Eq. (51) becomes

$$S_\psi(q,\tau) = \mathcal{S}^2(qW)\frac{2A^2}{\pi}\int d\mathbf{x}\, e^{i\mathbf{q}\cdot\mathbf{x}}\arcsin\left[\frac{S^0(x,\tau)}{S^0(0,\tau)}\right], \tag{52}$$

where, $S^0(x,\tau)$ is the linear structure factor of the time-dependent Ginzburg Landau equation and is given by

$$S^0(x,\tau) = e^{2(1-h_0+\nabla^2)\tau}S(x,0) . \tag{53}$$

The two-point correlation function for the $\delta h(\mathbf{x},\tau)$ field, i.e.,

$$S_{\delta h}(q,\tau)\equiv\langle \delta h(\mathbf{q},\tau)\delta h(-\mathbf{q},\tau)\rangle$$

can be evaluated using Eq. (50), i.e.,

$$S_{\delta h}(q,\tau)\approx \mathcal{S}^2(qW)4A^4W^2[\alpha'(e^{\beta_q\tau}-1)]^2 \times\int d\mathbf{x}\, e^{i\mathbf{q}\cdot\mathbf{x}}\Pi(x,\tau)\ , \tag{54}$$

where

$$\Pi(x,\tau)\equiv\langle |\nabla\psi^0(\mathbf{x},\tau)||\nabla\psi^0(0,\tau)|\delta(\psi^0(\mathbf{x},\tau))\delta(\psi^0(0,\tau))\rangle\ . \tag{55}$$

The explicit form of $\Pi(x,\tau)$ is given in Appendix C. The properties of the correlation functions will be the topic of the next two sections.

VIII. SCALING BEHAVIOR OF CORRELATION FUNCTIONS

The expressions for the correlation functions can be easily put into a scaling form in the asymptotic limit. Setting $Q=2q\tau^{1/2}$, the correlation functions become

$$S_\psi(q,\tau)=\tau^{d/2}f_\psi(Q)\mathcal{S}^2(QW/(2\tau^{1/2})) \tag{56}$$

and

$$S_{\delta h}(q,\tau)=\tau^{d/2-1}f_{\delta h}(Q)\mathcal{S}^2(QW/(2\tau^{1/2}))\ . \tag{57}$$

The scaling functions (f) for a random initial state [i.e., $S(q,0)=$const] are

$$f_\psi(Q)=\frac{2^{d+1}A^2}{\pi}\int d\mathbf{z}\, e^{i\mathbf{Q}\cdot\mathbf{z}}\arcsin(e^{-z^2/2}) \tag{58}$$

and

$$f_{\delta h}(Q)=2^dA^4W^2(e^{-RQ^2/4}-1)^2G(Q)\ , \tag{59}$$

where $G(Q)$ is given in Appendix C. In the late-time limit [i.e., $Q/(2\tau^{1/2})\ll W^{-1}$], the shaping functions are unity. Thus asymptotically,

$$S_\psi(q,\tau)=\tau^{d/2}f_\psi(Q)\ . \tag{60}$$

and

$$S_{\delta h}(q,\tau)=\tau^{d/2-1}f_{\delta h}(Q)\ . \tag{61}$$

The large-Q dependence of $S_\psi(q,\tau)$ is consistent with Porod's law [i.e., $S_\psi(q,\tau)\approx Q^{-d-1}$, for $Q\gg1$] as has been shown previously.[22(a)] The introduction of the shaping function implies this result is only valid when $q\ll W^{-1}$, thus Porod's law should be valid for wave vectors in the range $\tau^{-1/2}\ll 2q\ll W^{-1}$. Simply put, Porod's law is valid for wavelengths much larger than the domain-wall thickness, but much smaller than the average domain size. A more detail discussion of this effect will be given in the next section. A plot of the scaling function in a two-dimensional system is given in Fig. 6(a).

The large-Q dependence of $S_{\delta h}(q,\tau)$ can be found by writing

$$S_{\delta h}(q,\tau)=\tau^{d/2-1}\int d\mathbf{x}\, e^{i\mathbf{Q}\cdot\mathbf{x}}f_{\delta h}(x)\ , \tag{62}$$

which can be rewritten

$$S_{\delta h}(q,\tau)=\tau^{d/2-1}Q^{-d}\int d\mathbf{z}\, e^{iz\cdot Q/Q}f_{\delta h}(z/Q)\ . \tag{63}$$

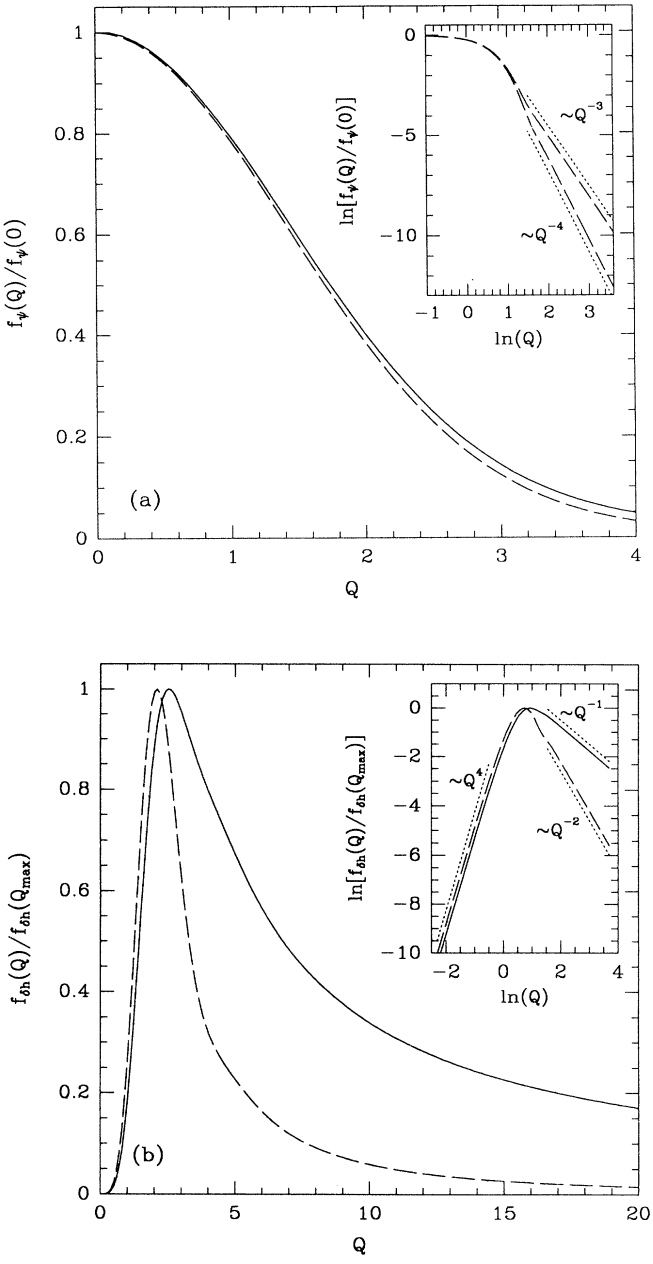

FIG. 6. Graphical depiction of the scaling functions in two and three dimensions. The solid line corresponds to $d=2$ and the dashed line corresponds to $d=3$. (a) The scaling function, $f_\psi(Q)$ as given in Eq. (58) in two and three dimensions. The inset depicts f_ψ on a logarithmic scale to highlight the large-Q dependence (i.e., Porod's law). (b) The scaling function, $f_{\delta h}$ as given in Eq. (59) for $R=1$ in two and three dimensions. The inset depicts f_ψ on a logarithmic scale to highlight the large- and small-Q dependences.

In the large-Q limit the scaling function is equivalent to (see Appendix C)

$$f_{\delta h}(x \to 0) \propto \frac{1}{x} . \tag{64}$$

Thus in the limit $\tau^{-1/2} \ll 2q \ll W^{-1}$,

$$S_{\delta h}(Q,\tau) \propto Q^{-d+1} . \tag{65}$$

It should be noted that this result implies that integrals over the δh correlation function are divergent in all dimensions. However, the nonscaling shaping function $\mathcal{S}(qW)$ decays exponentially in q as $q \to \infty$. Thus the shaping function provides a natural cutoff in Fourier space. The small-Q behavior can also be extracted in a similar manner, i.e.,

$$f_{\delta h}(Q) \propto Q^4 \int d\mathbf{x}\, g(x) , \tag{66}$$

or simply

$$f_{\delta h}(Q) \propto Q^4 \tag{67}$$

in the limit $Q \ll 1$. In Fig. 6(b) the $f_{\delta h}(Q)$ is graphically displayed for both two- and three-dimensional systems. It is interesting to note the dramatic asymmetry about the peak. This naturally occurs from the two limiting cases discussed above.

The two parameters in the initial dimensionless dynamical system (R and α') have significantly different influences on the domain growth. The coupling constant α' only affects the width of the interface and the amplitude of $S_{\delta h}(q,\tau)$, and consequently does not alter the scaling form of the correlation functions above. The influence of α' on the approach to scaling will be examined in the following section. In contrast to α', the parameter R (which is a ratio of the length and time scales of the two fields, h and ψ) does change the shape of scaling form of the h correlation function, but does not affect the approach to scaling. The rate at which the domain walls are formed (which is not included in this approximation) is, however, influenced by R. In Fig. 7 the form of $f_{\delta h}(Q)$ is displayed for various values of R.

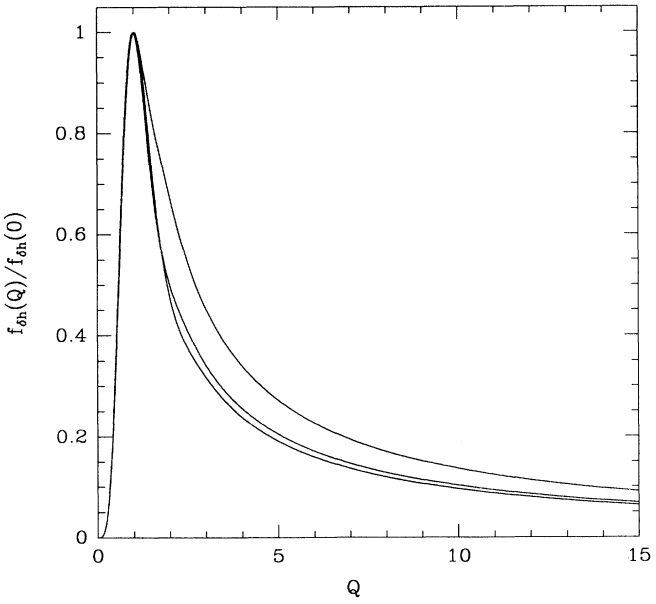

FIG. 7. Dependence of conserved field scaling function on the parameter R [see Eq. (11)] in $d=2$. From top to bottom the lines correspond to $R=1$, 2, and 3.

IX. APPROACH TO SCALING

In this section, the influence of the width of the domain walls or antiphase boundaries on the approach to the asymptotic scaling forms will be examined. The domain-wall thickness is a nonscaling length that reaches its asymptotic value exponentially in time. The creation of domain walls is not included in this theory, since it is a very early-time process. This restriction is unimportant except in the linear time regime (i.e., the regime in which exponential growth or decay is observed). Although the dynamical growth of the domain-wall shape is very rapid, the presence of a fixed nonscaling length will influence the shape of the correlation function when the domain sizes are not much larger than the domain width.

To qualitatively assess the influence of this nonscaling length on various quantities of interest, it is useful to expand the shaping function for small q's, i.e.,

$$\mathcal{S}^2(qW) \approx 1 - \frac{1}{3}\left[\frac{WQ\pi}{4\tau^{1/2}}\right]^2 + \frac{1}{15}\left[\frac{WQ\pi}{4\tau^{1/2}}\right]^4 - \frac{2}{189}\left[\frac{WQ\pi}{4\tau^{1/2}}\right]^6 + \cdots , \tag{68}$$

where $Q \equiv 2q\tau^{1/2}$. As an example, the moments of the correlation functions, which are commonly used to ascertain the dynamic growth exponent, will be determined. The moments of the $S_\psi(q,\tau)$ correlation function $[M_\psi^n(\tau)]$ are defined,

$$M_\psi^n(\tau) \equiv \int d\mathbf{q}\, q^n S_\psi(q,\tau) . \tag{69}$$

In light of Eqs. (69) and (56) this can be rewritten

$$M_\psi^n(\tau) = \tau^{-n/2}\left[C_\psi^n - \frac{1}{3}\left[\frac{W\pi}{2}\right]^2 \frac{C_\psi^{n+2}}{\tau^1} + \frac{1}{15}\left[\frac{W\pi}{2}\right]^4 \frac{C_\psi^{n+4}}{\tau^2} - \cdots\right] , \tag{70}$$

where

$$C_\psi^n \equiv \int d\mathbf{z}\, z^n f_\psi(2z) . \tag{71}$$

Similarly for the h field the moments can be written

$$M_{\delta h}^n(\tau) = \tau^{-n/2-1}\left[C_{\delta h}^n - \frac{1}{3}\left[\frac{W\pi}{2}\right]^2 \frac{C_{\delta h}^{n+2}}{\tau^1} + \frac{1}{15}\left[\frac{W\pi}{2}\right]^4 \frac{C_{\delta h}^{n+4}}{\tau^2} - \cdots\right] , \tag{72}$$

where

$$C^n_{\delta h} = \int dz\, z^n f_{\delta h}(2z) \ . \tag{73}$$

In Figs. 8(a) and 8(b) the first two moments [i.e., $n=1$ and 2)] are plotted versus time for the ψ and δh fields, respectively. The time taken to reach the asymptotic scaling exponent depends on the order (n) of the moment. The higher the order of the moment the slower the convergence to the asymptotic exponent, since large wave vectors contribute more to these moments. It is important to note that the moments of the correlation functions

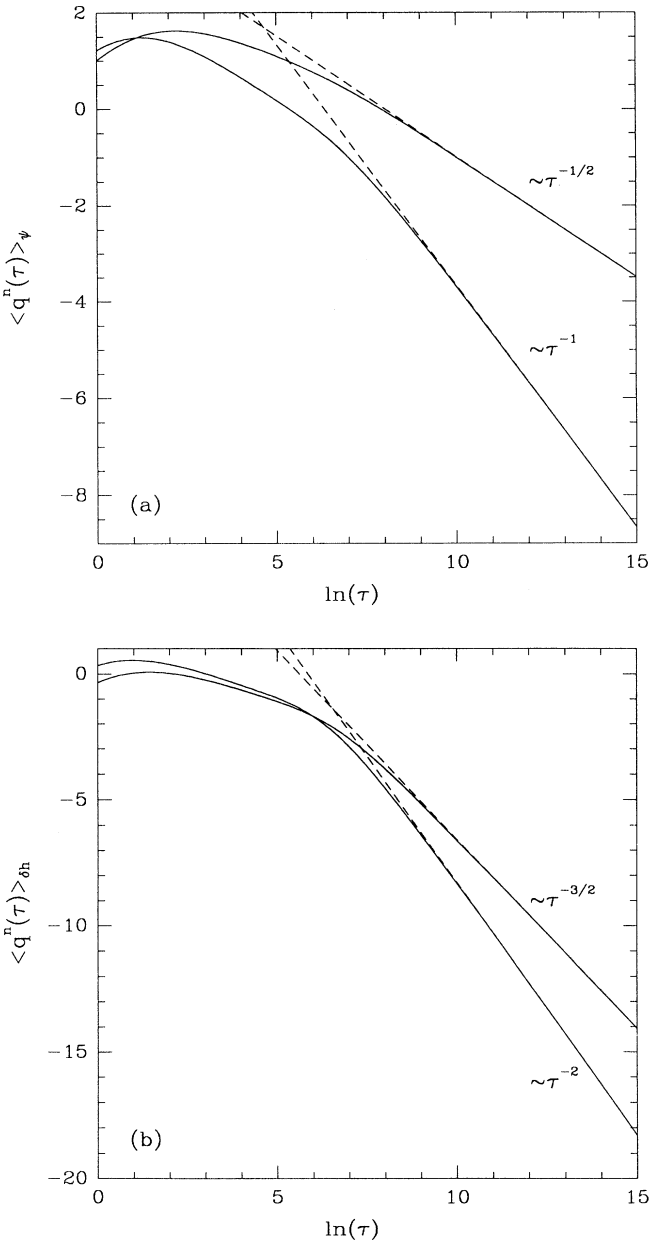

FIG. 8. Time dependence of moments of nonconserved and conserved fields in $d=2$. In both figures the value of the parameters α', h_0, and R are the same as in Fig. (4). (a) Approach of first two moments to asymptotic slopes as determined by Eq. (70) for ψ field. The top line is the first moment and the bottom line is the second moment. (b) Approach of first two moments to asymptotic slopes for δh field. The top line is the first moment and the bottom line is the second moment.

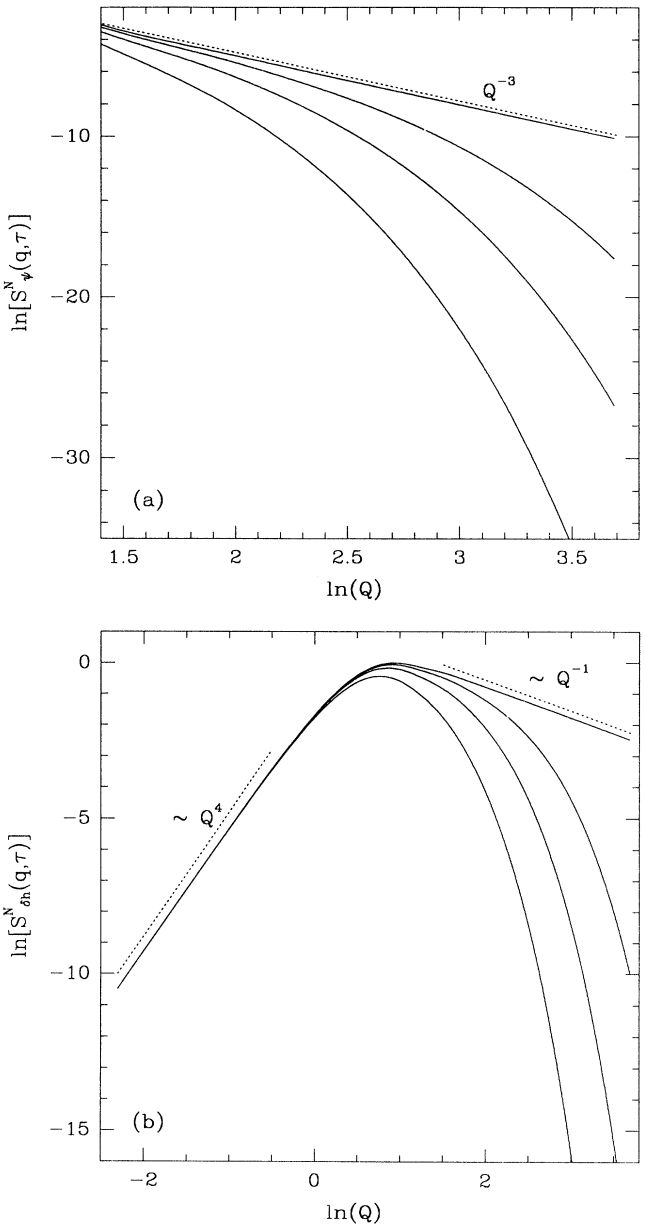

FIG. 9. Time dependence of long-and short-wavelength behavior of structure factors in $d=2$. In both figures the value of the parameters α', h_0, and R are the same as in Fig. 4. (a) Approach of nonconserved structure factor to Porod's law. The lines from bottom to top represent $\tau=10$, 30, 100, and the asymptotic scaling form [Eqs. (56) and (58)]. (b) Approach of conserved structure factor to short- and long-wavelength asymptotic values in $d=2$. The lines from bottom to top represent $\tau=10$, 30, 100, and the asymptotic scaling form [Eqs. (57) and (59)].

divided by the shaping function will scale at very early times (i.e., immediately following the linear regime).

The shaping function also has a major effect on the tails of the scaling function. In the previous section it was determined that $f_\psi(Q \gg 1) \approx Q^{-d-1}$ and $f_{\delta h} Q \gg 1) \approx Q^{-d+1}$. The early-time correction to these results can easily be obtained in a manner similar to that described above, i.e.,

$$f_\psi(Q \gg 1) \approx Q^{-d-1}\left[1-\frac{1}{3}\left[\frac{WQ\pi}{4\tau^{1/2}}\right]^2+\cdots\right], \tag{74}$$

$$f_{\delta h}(Q \gg 1) \approx Q^{-d+1}\left[1-\frac{1}{3}\left[\frac{WQ\pi}{4\tau^{1/2}}\right]^2+\cdots\right]. \tag{75}$$

In Figs. 9(a) and 9(b) the approach to scaling in the tails is examined for the ψ and δh field, respectively. From these figures, it can clearly be seen that a finite W causes deviation from the asymptotic scaling results. As in the case of the moments, the scaling form of the tails can be obtained from experimental data at early times, by dividing the structure factor by the shaping function.

X. CONCLUSIONS

In summary, this paper has provided experimentally testable predictions for the growth of domains in an order-disorder transition in the presence of coupling to a conserved field. The main predictions are the scaling functions $f_\psi(Q)$ and $f_{\delta h}(Q)$ and a growth exponent of $\frac{1}{2}$. The scaling functions predict tails of Q^{-d-1} and Q^{-d+1}, respectively. In addition the approach to these asymptotic results can be examined through Eqs. (74) and (75), which predict corrections of the order Q^2W^2/τ. Of greater interest is the predictions for the moments and growth exponents. Again, experimental or numerical results can easily be compared with the results given in Eqs. (70) and (72). Perhaps one of the most interesting results is the influence of the domain-wall thickness on the approach to scaling. By dividing the correlation functions by the shaping function, scaling should be observed during times where the domain sizes are not asymptotically larger than the domain walls.

ACKNOWLEDGMENTS

The authors would like to thank Dr. Mark Sutton for useful discussions. The research was kindly supported by the Natural Sciences and Engineering Research Council of Canada and les Fonds pour la Formation de Chercheurs et l'Aide à la Recherche de la Province de Québec.

APPENDIX A

An estimate of the coupling constant α' can be obtained by using a nearest- and next-nearest-neighbor approximation (i.e., a Bragg-Williams approximation) for the free energy and adding a strain energy. In this approach[7] $\mathcal{F}$ becomes

$$\begin{aligned}\frac{\mathcal{F}}{N_v} &= \{[c(1-c)+\phi^2]V_1+[c(1-c)-\phi^2]V_2\} \\ &+\frac{k_BT}{2}[(c+\phi)\ln(c+\phi)+(1-c-\phi)\ln(1-c-\phi)+(c-\phi)\ln(c-\phi)+(1-c+\phi)\ln(1-c+\phi)] \\ &+Y[\epsilon_c\delta c+\epsilon_\phi\phi^2)^2],\end{aligned}$$

where Y is Young's modulus, k_B is Boltzmann's constant, T is temperature, and N_v is the number of atoms per unit volume. V_i is the interchange energy defined as $V_i \equiv E_i^{AB}-(E_i^{AA}+E_i^{BB})/2$, where E_i are the atomic interaction strengths and the index i is 1 for nearest neighbors and 2 for next-nearest neighbors. The quantities ϵ_c and ϵ_ϕ are elastic constants defined by expanding the lattice parameter (a) on the c_λ line [i.e., $a \approx a'(1+\epsilon_c\delta c+\epsilon_\phi\phi^2+\cdots)$]. These parameters can be measured by determining the slope of a lattice parameter versus composition curves above and below this line.

Expanding around $\delta c = 0$ (where, $c \equiv c_0+\delta c$) and $\phi = 0$ gives

$$\begin{aligned}\mathcal{F} \approx \mathcal{F}(c_0,0)&+\frac{\phi^2}{2}\left[\frac{N_vk_BT}{c_0(1-c_0)}+2N_v(V_1-V_2)\right]+\frac{\phi^4}{4}\left[\frac{N_vk_BT}{3}\left[\frac{1}{c_0^3}+\frac{1}{(1-c_0)^3}\right]+4\epsilon_\phi^2Y\right] \\ &+\frac{\phi^2\delta c}{2}\left[N_vk_BT\left[\frac{1}{(1-c_0)^2}-\frac{1}{c_0^2}\right]+4\epsilon_\phi\epsilon_cY\right]+\frac{(\delta c)^2}{2}\left[\frac{N_vk_BT}{c_0(1-c_0)}-2N_v(V_1+V_2)+2\epsilon_c^2Y\right].\end{aligned} \tag{A1}$$

The term proportional to δc is not included since it does not contribute to the equation of motion for either field. Under these assumptions the coupling constant is

$$\alpha' = \frac{(2c-1+4c^2C^2\epsilon_c\epsilon_\phi Y')^2}{2\{1+cC[2\epsilon_c^2Y'-2(V_1'+V_2')]\}[(C^3+c^3)/3+4c^3C^3\epsilon_\phi^2Y']}, \tag{A2}$$

where $C \equiv 1-c$, $Y' = Y/(N_vk_BT)$, and $V_i' = V_i/(k_BT)$. The various parameters in Eq. (A2) can be measured experimentally. Allen and Cahn[7(a)] have provided estimates of several of these parameters for the Fe-Al system. Specifically, $Y' \approx 463$ K/T, $\epsilon_\phi \approx -0.22$, $\epsilon_c \approx 0.45$, and $V_1'+V_2' \approx 175$ K/T. These parameters were used to construct Fig. 1.

APPENDIX B

The first-order correction term C_1 to Eq. (32) is

$$C_1=\alpha'\beta_q e^{(-\beta_q\tau)v}\tau\int_0^1 e^{-\beta_q\tau}dv\left[\frac{\delta}{\delta v}\int d\mathbf{x}\,e^{i\mathbf{q}\cdot\mathbf{x}}\psi^2(\mathbf{x},\tau v)\right]_{v=1}(v-1)\ . \tag{B1}$$

Using Eq. (29) for ψ the derivative in Eq. (B1) becomes

$$\left[\frac{\delta}{\delta v}\int d\mathbf{x}\,e^{i\mathbf{q}\cdot\mathbf{x}}\psi^2(\mathbf{x},\tau v)\right]_{v=1}=2\tau\int d\mathbf{x}\,e^{i\mathbf{q}\cdot\mathbf{x}}\psi(\mathbf{x},\tau)\frac{\delta\psi(\mathbf{x},\tau)}{\delta\tau}$$

$$\approx 2\tau\int d\mathbf{x}\,e^{i\mathbf{q}\cdot\mathbf{x}}\frac{\psi^0(\mathbf{x},\tau)\gamma\psi^0(\mathbf{x},\tau)}{\{1+[\psi^0(\mathbf{x},\tau)]^2\}^2}\ . \tag{B2}$$

Substituting this result into Eq. (B1) and evaluating the integrals over dv, the correction term becomes

$$C_1\approx 2\alpha'[(1-\beta_q\tau)e^{\beta_q\tau}-1]\int d\mathbf{x}\,e^{i\mathbf{q}\cdot\mathbf{x}}\left[\frac{\psi^0(\mathbf{x},\tau)\gamma\psi^0(\mathbf{x},\tau)}{\{1+[\psi^0(\mathbf{x},\tau)]^2\}^2}\right]\ . \tag{B3}$$

Since $\psi^0(\mathbf{x},\tau)\approx e^{(1-h_0)\tau}$, in the late-time long-wavelength limit, this becomes

$$C_1\propto e^{-2(1-h_0)\tau}\ . \tag{B4}$$

Thus the correction term to Eq. (32) decays exponentially in time, and is asymptotically negligible.

APPENDIX C

The correlation function given in Eq. (55) can be evaluated in a manner similar to that used by Ohta, Jasnow, and Kawasaki[6] to obtain the area density in model A. Specifically the correlation function can be written (for $d\geq 2$)

$$\Pi(x,\tau)=\int d\mathbf{q}_1\int d\mathbf{q}_2\int\frac{d\mathbf{r}_1}{(2\pi)^d}\frac{d\mathbf{r}_2}{(2\pi)^2}\frac{e^{i(\mathbf{q}_1\cdot\mathbf{r}_1+\mathbf{q}_2\cdot\mathbf{r}_2)}}{|\mathbf{r}_1||\mathbf{r}_2|}\int_{-\infty}^{\infty}\frac{d\lambda_1}{2\pi}\int_{-\infty}^{\infty}\frac{d\lambda_2}{2\pi}\nabla_{q_1}^2\nabla_{q_2}^2$$

$$\times\langle\exp\{i[\lambda_1\psi^0(\mathbf{x}_1,\tau)+\lambda_2\psi^0(\mathbf{x}_2,\tau)+\mathbf{q}_1\cdot\nabla\psi^0(\mathbf{x}_1,\tau)+\mathbf{q}_2\cdot\nabla\psi^0(\mathbf{x}_2,\tau)]\}\rangle \tag{C1}$$

where $x\equiv|\mathbf{x}_1-\mathbf{x}_2|$. Since the field variables ψ^0 are Gaussian, the correlation of the exponential can be written as an exponential of the correlation of the square of the argument of the exponential, i.e.,

$$\langle\exp\{i[\lambda_1\psi^0(\mathbf{x}_1,\tau)+\lambda_2\psi^0(\mathbf{x}_2,\tau)+\mathbf{q}_1\cdot\nabla\psi^0(\mathbf{x}_1,\tau)+\mathbf{q}_2\cdot\nabla\psi^0(\mathbf{x}_2,\tau)]\}\rangle$$

$$=\exp\{-\tfrac{1}{2}[(\lambda_1^2+\lambda_2^2)\beta_0(\tau)+2\lambda_1\lambda_2 S^0(x,\tau)+2(\lambda_2\mathbf{q}_1-\lambda_1\mathbf{q}_2)\cdot\nabla S^0(x,\tau)+(q_1^2+q_2^2)\beta_2(\tau)-2\mathbf{q}_1\mathbf{q}_2:\nabla\nabla S^0(x,\tau)]\}\ , \tag{C2}$$

where

$$S^0(x,\tau)\equiv\langle\psi^0(\mathbf{x}_1,\tau)\psi^0(\mathbf{x}_2,\tau)\rangle\ , \tag{C3}$$

$$\psi^0(\mathbf{x},\tau)\equiv e^{\gamma\tau}\psi(\mathbf{x},0)\ , \tag{C4}$$

$$\beta_2(\tau)\equiv\int d\mathbf{k}\,k_x^2 S^0(k,\tau)\ , \tag{C5}$$

and

$$\beta_0(\tau)\equiv\int d\mathbf{k}\,S^0(k,\tau)\ . \tag{C6}$$

Evaluation of the λ_i and $\mathbf{r}_i$ integrals leads to the following equation:

$$\Pi(x,\tau)=C_d'\frac{\beta_2}{\sin\theta\beta_0}\int d\mathbf{q}_1\int d\mathbf{q}_2(q_1q_2)^{-d+1}\nabla_{q_1}^2\nabla_{q_2}^2$$

$$\times\exp\left\{-\frac{1}{2}\left[(\vec{\mathbf{q}}_1^2+\vec{\mathbf{q}}_2^2):\left[\overleftrightarrow{\mathbf{I}}-\frac{[\nabla S^0(x,\tau)]^2}{\beta_0\beta_2\sin^2\theta}\right]\right.\right.$$

$$\left.\left.-2\mathbf{q}_1\mathbf{q}_2:\left[\frac{\nabla\nabla S^0(x,\tau)}{\beta_2}+\frac{[\nabla S^0(x,\tau)]^2}{\beta_2\beta_0\sin^2\theta}\cos\theta\right]\right]\right\} \tag{C7}$$

where, $\cos\theta \equiv S^0(x,\tau)/\beta_0$, $C_d \equiv (2\sqrt{\pi})^{d-1}\Gamma((d-1)/2)$, $\overleftrightarrow{\mathbf{I}}$ is the unit tensor and the $C_d' \equiv (C_d)^2/(2\pi)^{2d+1}$. This can be further simplified by explicitly calculating β's and $S^0(x,\tau)$ and making the variable change $R = x/(2\tau^{1/2})$. In Fourier space the result is

$$\Pi(Q,\tau) = \tau^{d/2-1}\int d\mathbf{R} e^{i\mathbf{R}\cdot\mathbf{Q}} G(R) \tag{C8}$$

where

$$G(R) \equiv \frac{C_d'}{(1-e^{-R^2})^{1/2}} \int d\mathbf{q}_1 \int d\mathbf{q}_2 (q_1 q_2)^{-d+1} \nabla_{q_1}^2 \nabla_{q_2}^2 \times \exp\left\{ -\frac{1}{2}\left[(\mathbf{q}_1^2+\mathbf{q}_2^2) : \left[\overleftrightarrow{\mathbf{I}} - \frac{(\mathbf{R})^2}{e^{R^2}-1} \right] + 2\mathbf{q}_1\mathbf{q}_2 : \left[\overleftrightarrow{\mathbf{I}} - \frac{\mathbf{R}^2}{1-e^{-R^2}} e^{-R^2/2} \right] \right] \right\} \tag{C9}$$

In the short-wavelength limit, the $\mathbf{q}_i$ integrals equal $1/C_d'$, thus

$$G(R \ll 1) \approx R^{-1} \tag{C10}$$

in all dimensions.

The above expression is valid for $d \geq 2$, and can be further reduced by evaluating the radial part of the integrals. The angular parts must be integrated numerically, however, these calculations need only be done once for all times, since this piece scales. In $d=2$, $G(r)$ becomes

$$G^{2d}(R) \equiv \frac{C_d'}{(1-e^{-R^2})^{1/2}} \int_0^{2\pi} d\phi_1 \int_0^{2\pi} d\phi_2 \left[\sqrt{c_1 c_2 - c_3^2}\, \arccos\left[\frac{c_3}{\sqrt{c_1 c_2}} \right] - \frac{c_3}{2} \arccos^2\left[\frac{c_3}{\sqrt{c_1 c_2}} \right] \right], \tag{C11}$$

where

$$c_1 \equiv 1 - a\sin^2\phi_1 , \tag{C12}$$

$$c_2 \equiv 1 - a\sin^2\phi_2 , \tag{C13}$$

$$c_3 \equiv b_1(\cos\phi_1\cos\phi_2 + b_2\sin\phi_1\sin\phi_2) , \tag{C14}$$

$$a \equiv R^2/(e^{R^2}-1) , \tag{C15}$$

$$b_1 \equiv e^{-R^2/2} , \tag{C16}$$

$$b_2 \equiv 1 - R^2/(1-e^{-R^2}) . \tag{C17}$$

In $d=3$, $G(R)$ is

$$G^{3d}(R) \equiv \frac{C_d'}{(1-e^{-R^2})^{1/2}} \int_0^{2\pi} d\phi \int_0^{\pi} d\theta_1 \sin\theta_1 \int_0^{\pi} d\theta_2 \sin\theta_2 \left[\sqrt{d_1 d_2 - d_3^2}\, \arccos\left[\frac{d_3}{\sqrt{d_1 d_2}} \right] - \frac{d_3}{2} \arccos^2\left[\frac{d_3}{\sqrt{d_1 d_2}} \right] \right], \tag{C18}$$

where

$$d_1 \equiv 1 - a\cos^2\theta_1 , \tag{C19}$$

$$d_2 \equiv 1 - a\cos^2\theta_2 , \tag{C20}$$

$$d_3 \equiv b_1[\cos\theta_1\cos\theta_2 b_2 + \sin\theta_1\sin\theta_2\cos(\phi)] . \tag{C21}$$

[1] J. D. Gunton, M. San Miguel, and P. Sahni, in *Phase Transitions and Critical Phenomena,* edited by C. Domb and J. L. Lebowitz (Academic, New York, 1983), Vol. 8, pp. 267, and references therein.

[2] P. C. Hohenberg and B. I. Halperin, Rev. Mod. Phys. **49**, 435 (1977); B. I. Halperin, P. C. Hohenberg, and S.-k. Ma, Phys. Rev. B **10**, 139 (1974); **13**, 4119 (1976).

[3] J. D. Gunton and M. Droz, *Introduction to the Theory of Metastable and Unstable States* (Springer-Verlag, Berlin, 1983).

[4] K. Kawasaki, M. C. Yalabik, and J. D. Gunton, Phys. Rev. A **17**, 455 (1978).

[5] R. K. P. Zia, R. Bausch, H. K. Janssen, and V. Dohm, Mod. Phys. Lett. B **2**, 961 (1988). See also L. Jorgenson, R. Harris, and M. Grant, Phys. Rev. Lett. **63**, 1693 (1989); R. Bausch, V. Dohm, H. K. Janssen, and R. K. P. Zia, Z. Phys. B **82**, 121 (1991).

[6] T. Ohta, D. Jasnow, and K. Kawasaki, Phys. Rev. Lett. **49**, 1223 (1982); T. Ohta, Ann. Phys. (N.Y.) **158**, 31 (1984).

[7] (a) S. M. Allen and J. W. Cahn, Acta Metall. **23**, 1 (1975); (b) **24**, 425 (1976); (c) **27**, 1085 (1979).

[8]Y. Oono and S. Puri, Phys. Rev. Lett. **58**, 836 (1987); Phys. Rev. A **38**, 1542 (1988); Mod. Phys. Lett. B **2**, 861 (1988).
[9]W. W. Mullins and J. Viñals, Acta. Metall. **37**, 991 (1989).
[10]A. Sadiq and K. Binder, J. Stat. Phys. **35**, 517 (1984).
[11]S. M. L. Sastry and H. A. Lipsitt, Metal. Trans. **8A**, 1543 (1977).
[12]M. Seki and D. E. Mikkola, Metal. Trans. **2**, 1635 (1971); C. L. Rase and D. E. Mikkola, *ibid.* **6A**, 2267 (1975).
[13]C. Roland and M. Grant, Phys. Rev. B **41**, 4663 (1990).
[14]S. E. Nagler, R. F. Shannon, Jr., C. R. Harkless, M. A. Singh, and R. M. Nicklow, Phys. Rev. Lett. **61**, 718 (1988).
[15]M. Laradji, M. Grant, M. J. Zuckermann, and W. Klein, Phys. Rev. B **41**, 4646 (1990).
[16]B. D. Gaulin, S. Spooner, and Y. Morii, Phys. Rev. Lett. **59**, 668 (1987).
[17]C. Roland and M. Grant, Phys. Rev. Lett. **60**, 2657 (1988); Phys. Rev. B **39**, 11 971 (1989).
[18]E. T. Gawlinski, J. Viñals, and J. D. Gunton, Phys. Rev. B **39**, 7266 (1989); R. Toral, A. Chakrabarti, and J. D. Gunton, Phys. Rev. Lett. **60**, 2311 (1988); R. Toral, A. Chakrabarti, and J. D. Gunton, Phys. Rev. B **39**, 901 (1989).
[19]T. M. Rogers, K. R. Elder, and R. C. Desai, Phys. Rev. B **37**, 9638 (1988); T. M. Rogers and R. C. Desai, *ibid.* **39**, 11 956 (1989).
[20]C. M. Bender and S. A. Orzag, *Advanced Mathematical Methods for Scientists and Engineers* (McGraw-Hill, New York, 1978).
[21]M. Suzuki, Prog. Theor. Phys. **56**, 77 (1976); **56**, 477 (1976); J. Stat. Phys. **16**, 11 (1977).
[22]A general class of dynamical systems is considered in (a) K. R. Elder and M. Grant, J. Phys. A **23**, L803 (1990); specific applications have been made for the Fischer Kolmogorov equation, (b) S. Puri, K. R. Elder, and R. C. Desai, Phys. Lett. A **142**, 357 (1989); a magnetic bubble system, (c) C. Roland and R. C. Desai, Phys. Rev. B **42**, 6658 (1990); and a model of the visual cortex, (d) B. Cowen, R. Thompson, M. Zuckerman, M. Grant, and K. Elder (unpublished).
[23]G. Porod, in *Small Angle X-Ray Scatterings,* edited by O. Glatter and O. Kratsky (Academic, New York, 1982).
[24]K. F. Ludwig, Jr., G. B. Stephenson, J. L. Jordan-Sweet, J. Mainville, Y. S. Yang, and M. Sutton, Phys. Rev. Lett. **61**, 1859 (1988).
[25]D. J. Bergman and B. I. Halperin, Phys. Rev. B **13**, 2145 (1976).
[26]D. R. Nelson and M. E. Fisher, Phys. Rev. B **11**, 1030 (1975).
[27]G. F. Mazenko, O. T. Valls, and M. Zannetti, Phys. Rev. B **38**, 520 (1988); G. F. Mazenko, Phys. Rev. Lett. **63**, 1605 (1989).
[28]P. S. Sahni, J. D. Gunton, S. L. Katz, and R. H. Timpe, Phys. Rev. B **25**, 389 (1982); P. S. Sahni and J. D. Gunton, Phys. Rev. Lett. **43**, 369 (1980).
[29]M. San Miguel and J. D. Gunton, Phys. Rev. B **23**, 2317 (1981); M. San Miguel, G. Dee, J. D. Gunton, and P. S. Sahni, *ibid.* **23**, 2334 (1981).